

PRKAA1, stabilized by FTO in an m⁶A-YTHDF2-dependent manner, promotes cell proliferation and glycolysis of gastric cancer by regulating the redox balance

Yangmei ZHANG^{1,2,3,4,*}, Xichang ZHOU^{5,*}, Xue CHENG^{6,*}, Xiu HONG⁷, Xiaowei JIANG⁸, Guilong JING⁸, Kai CHEN^{1,*}, Yang LI^{7,*}

¹Department of Medical Oncology, The First Affiliated Hospital of Soochow University, Suzhou, China; ²Xuzhou Institute of Medical Sciences, Xuzhou, China; ³Department of Cancer Rehabilitation, Xuzhou Central Hospital, The Xuzhou Clinical College of Xuzhou Medical University, Xuzhou, China; ⁴Xuzhou Rehabilitation Hospital, The Affiliated Xuzhou Rehabilitation Hospital of Xuzhou Medical University, Xuzhou, China; ⁵Department of Intervention, Xuzhou Central Hospital, The Xuzhou Clinical College of Xuzhou Medical University, Xuzhou, China; ⁶Department of Oncology, Yancheng Third People's Hospital, Yancheng, China; ⁷Department of Central Laboratory, Xuzhou Central Hospital, The Xuzhou Clinical College of Xuzhou Medical University, Xuzhou, China; ⁸Department of Rehabilitation Medicine, Xuzhou Central Hospital, The Xuzhou Clinical College of Xuzhou Medical University, Xuzhou, China

*Correspondence: kaichen0612@163.com, yangli211214@163.com

*Contributed equally to this work.

Received July 14, 2022 / Accepted October 18, 2022

Gastric carcinoma (GC) is the fourth most common malignancy worldwide and the second cause of death of all malignancies worldwide. AMPK catalytic subunit $\alpha 1$ (PRKAA1) is involved in various types of cancer and PRKAA1 knock-down significantly decreased the invasiveness of GC cells. Fat mass and obesity-associated protein (FTO)-regulation of m⁶A has been shown to be involved in different diseases including cancer. However, the role of PRKAA1 and m⁶A modification in GC remains to be elucidated. PRKAA1 was silenced or overexpressed to study the role of PRKAA1 in regulating cell viability, colony formation, and glycolysis. Levels of lactic acid, GSH, and NADP⁺/NADPH were measured using commercial kits. Extracellular acidification rates were determined by an extracellular flux analyzer. RNA immunoprecipitation was performed to test m⁶A levels and the interaction between PRKAA1-3'-UTR and YTHDF2. Quantitative RT-PCR and immunoblots were applied to measure mRNA or protein levels, respectively. PRKAA1 silencing inhibited cell growth, colony formation, and glycolysis but enhanced apoptosis, while the PRKAA1 overexpression promoted cell growth, colony formation, and glycolysis but inhibited apoptosis of GC cells. Data also indicated that PRKAA1 regulated cell growth and apoptosis by regulating the redox balance. Mechanism study demonstrated that FTO regulated PRKAA1 mRNA m⁶A modification and stability. Clinical samples analysis demonstrated that PRKAA1 and FTO expression were increased in GC patients and positively correlated with each other. FTO increased levels of PRKAA1 by regulating its mRNA m⁶A modification and stability. PRKAA1, in turn, promoted cell viability, colony formation, and glycolysis but inhibited apoptosis of GC cells by promoting the redox balance.

Key words: redox balance, N⁶-methyladenosine, gastric carcinoma, PRKAA1, glycolysis, apoptosis

Gastric carcinoma (GC) is the 4th malignancy and the 2nd cause of death of all malignancies worldwide [1]. Although the incidence of GC is decreasing due to medical advances, it still carries a poor prognosis [2]. Although GC is highly treatable in its early stages, advanced GC has a median survival of just ~9–10 months [3]. The overall survival is about 31% in the USA and 25% worldwide [4]. The reasons for the low survival include late diagnosis, chemoresistance, etc. [4, 5]. Risk factors include age, sex, race, infection with *Helicobacter pylori*, and smoking [6].

Cancer is heterogeneous and various cancers use glycolysis and/or oxidative phosphorylation for energy metabolism. The cell survival, proliferation, invasion, metastasis, and drug resistance of GC are energy-demanding processes, fuelled by glycolysis and oxidative metabolism [7]. Compared to normal cells, cancer cells have a higher demand on the mitochondrial respiratory chain to generate more ATP for their rapid growth and differentiation, thus inevitably making cancer cells have high levels of endogenous oxidative stress [8]. The imbalance in ROS generation and removal

causes excessive accumulation of ROS and thus oxidative stress, resulting in detrimental oxidative DNA damage, which is regarded as a major factor for carcinogenesis [9]. Controlling ROS metabolism is beneficial for the prevention and treatment of cancer. The different redox states between normal and cancer cells would provide an opportunity to selectively induce cancer cell death. AMPK, comprised of α -, β -, and γ -subunit, is involved in the regulation of glucose and lipid metabolism [10]. The α -subunit has two isoforms, $\alpha 1$ (PRKAA1) or $\alpha 2$ (PRKAA2). AMPK activation increases the energy supply [11]. Studies show that PRKAA1 is involved in different types of cancer, including GC. For instance, genetic variations in PRKAA1 predict the risk and progression of GC [12]. PRKAA1 was implicated in the hypoxia-induced proliferation, migration, invasion, and glycolysis of GC cells [13]. Our previous studies have shown that PRKAA1 regulates the proliferation, apoptosis, invasion, and migration of GC cells via the JNK1, AKT, or NF- κ B signaling pathway [14, 15]. However, its role in regulating glycolysis and redox balance and the possible mechanism involved have not been fully elucidated and need to be further studied.

RNA N⁶-methyladenosine (m⁶A), the most prevalent internal modification in eukaryotic mRNA [16, 17], is a regulatory mechanism for tumor progression in different types of cancer [18]. For example, it has been reported that suppressing m⁶A modification in myeloid cells significantly increased tumor growth [19]. Zhang et al. have demonstrated that the reduction of m⁶A mRNA contributed to the aggressiveness of lung cancer [20]. Fat mass and obesity-associated protein (FTO), a demethylase for N⁶-methyladenosine modification, has been shown to be involved in different biological processes. For example, AMPK controls lipid metabolism in skeletal muscle via FTO-dependent m⁶A demethylation [16]. Yang et al. have reported that FTO demethylation promotes melanoma growth [21]. However, the underlying regulatory mechanisms of m⁶A mRNA demethylation in GC remain unknown.

Therefore, we aim to explore the role of m⁶A mRNA demethylation of PRKAA1 in the growth and apoptosis of GC cells.

Patients and methods

Patient information. Thirty GC or adjacent tissues were collected with informed consent obtained. The inclusion criteria were defined as a certain diagnosis of GC. Also, patients who had received any treatment such as chemotherapy, radiotherapy, and biological medication (monoclonal antibodies) before the sampling were excluded from the study. This study had the approval of the ethics committee of Xuzhou Central Hospital. All the research was carried out according to provisions of the Declaration of Helsinki of 1975. The GC tissue microarray including 126 GC tissues was purchased from Shanghai Outdo Biotech (China).

Immunohistochemistry (IHC). Tissues were embedded, sectioned, and stained with anti-PRKAA1 antibody (Abcam, ab32047), anti-FTO antibody (Abcam, ab126605), followed by HRP-conjugated secondary antibody. Results were evaluated by two independent pathologists. Results were scored by the H-score system (positively stained cells: 0–4, intensity of staining: 0–3). Patients were separated into low or high expression group (score <6 or score >6).

Cell culture. MKN-45, BGC-823, and MGC-803 cells were purchased from the Chinese Academy of Science. Cells were cultured in DMEM or RPMI-1640 with 10% FBS with or without N-acetyl-cysteine (NAC; 5 mM; Selleck Chemicals, TX, USA).

Gene knockdown or overexpression. Protocols were mentioned previously [22]. shRNAs for PRKAA1 (shPRKAA1#1, GGTAGATATATGGAGCAGT; shPRKAA1#2, ATGAGTCTACAGTTATACC), FTO (shFTO#1, GGAGCTCATAAAGAGGTT; shFTO#2, CCTGAACACCAGGCTCTTT), or YTHDF2 (shYTHDF2#1, GCACAGAAAGTTGCAAGCAA; shYTHDF2#2, GCACAGAGCATGGTAACAA) were inserted into the pLKO.1 plasmid. To overexpress PRKAA1 or FTO, coding sequences were inserted into the pLVX-Puro plasmids. 293T cells were transfected for 48 h, cells were then used to collect the virus.

Cell viability assay. Cells in 96-well plates were treated for 0 h, 12 h, 24 h, or 48 h, then CCK-8 was added for 1 h, and OD450 was recorded.

Colony formation assay. Cells were treated and cultured in dishes for 2 weeks. At the end of the incubation, colonies were fixed with paraformaldehyde for 15 min and stained with 0.5% crystal violet for 30 min. Colonies (>50 cells) were quantified.

Cell apoptosis assay. Cells were collected 48 h after treatment. The staining procedures followed two steps: 1) 20 min of incubation with Annexin-V-FITC at 4°C and 2) another 20 min of incubation with propidium iodide (PI). An Accuri™ C6 flow cytometer was then used to examine cell apoptosis.

Extracellular flux analysis. Extracellular acidification rate (ECAR) was measured with an XF24 Extracellular Flux Analyzer [23]. Briefly, cells digested to a density of 1×10^4 /well, were seeded in XF-24 culture plates (Agilent Technologies, Santa Clara, CA, USA), and were then placed in an incubator of 37°C and 5% CO₂ for 24 h. Around 1 h before detection, the culture medium was replaced by XF Base Medium (Agilent Technologies). Subsequently, the cells were treated sequentially with 1 μ M of glucose, 1 μ M of oligomycin, (ATP synthase inhibitor), and 0.5 μ M of 2-DG (the glycolytic inhibitor) at time points for measurement of ECAR.

Measurement of lactic acid, GSH, and NADP+/NADPH. The cells were seeded in 96-well plates at 3.5×10^3 cells/well. After overnight incubation at 37°C, 5% CO₂, the complete medium was changed to fresh DMEM (50 μ l/well). After 24 h, the supernatant of cells was collected by centrifugation. Then, according to the manufacturer's instructions, the lactic

acid release was determined using the Lactic Acid Assay Kit (Nanjing Jiancheng Bioengineering Institute, China). The GSH and NADP⁺/NADPH levels were determined by Reduced Glutathione (GSH) Assay Kit (Nanjing Jiancheng) and NADP/NADPH Assay Kit (Colorimetric) (Abcam; ab65349), respectively.

Quantitative RT-PCR (RT-qPCR). RNA from GC tissues and cell lines was isolated with TRIzol and used for the synthesis of first-strand cDNA. RT-qPCR was done using the SYBR Green kit. Primers (5′–3′) were listed: PRKAA1-F: CACAGAGATCGGGATCAGTTAG, PRKAA1-R: GGAGTTAGGTCAACAGGAGAAG; FTO-F: ACCTCCAGCAT-TAGATTC, FTO-R: GAAACTACCGCATTTACC; YTHDF2-F: ACACATTCGCCTAGAGAAC, YTHDF2-R: TATTTCCCACGACCTTGAC.

Immunoblots. Proteins from GC cells were isolated, separated by 10% SDS-PAGE, immunoblotted to PVDF membranes, blocked, and incubated with the following antibodies overnight at 4°C (PRKAA1, ab32047; FTO, ab126605; YTHDF2, ab220163 all from Abcam; GAPDH, 5174, Cell Signaling Technology). Then, incubated with the secondary antibody. ECL was used for image visualization. The density of the protein band was quantified by ImageJ.

Analysis of m⁶A. TRIzol reagent was used to extract the total RNA. Poly(A)⁺ RNA was purified using the GenElute™ mRNA Miniprep Kit (MRN10, Sigma, Louis, MO, USA). The m⁶A content was assayed using the m⁶A RNA Methylation Assay Kit (ab185912, Abcam). Briefly, 80 µl of binding solution and 200 ng of sample RNA were added into each designated well and then incubated at 37°C for 90 min for RNA binding. Each well was washed three times with the washing buffer. 50 µl of the diluted capture antibody was added into each well and then incubated at room temperature for 60 min. Each well was incubated with a detection antibody and enhancer solution at room temperature for 30 min subsequently. Finally, the wells were incubated with developer solution in the dark for 1–10 min at 25°C. The reaction was stopped with stop solution and determined using a microplate reader at 450 nm wavelength within 2 to 10 min.

Luciferase reporter assay. The 3′-UTR of PRKAA1 was cloned into the pGL3 vector (Promega, Madison, WI, USA). GC cells transduced with FTO shRNA or expression plasmids were transfected with the pGL3-PRKAA1 3′-UTR luciferase reporter plasmid and the pRL-TK vector (Promega) expressing the Renilla luciferase using Lipofectamine 2000 (Invitrogen). Luciferase activity was measured 48 h after transfection.

mRNA stability. Cells were treated with actinomycin D (0.2 mM) for 0, 3, and 6 h. The samples were then collected for total RNA extraction and cDNA synthesis, which were performed according to the methods described above. RT-qPCR was used to quantify mRNA.

RNA immunoprecipitation (RIP) assay. Magna RIP RNA-Binding Protein Immunoprecipitation kit (Milli-

pore Sigma, Burlington, MA, USA) was used for the RIP assay following the manufacturer's instructions. Cells were prepared using RIP lysis buffer and the RNA-protein complexes were conjugated with anti-m6A (ab208577), anti-YTHDF2 (ab246514), or anti-IgG antibody (ab172730, all from Abcam) overnight at 4°C, and washed with RIP-wash buffer for 10 min at 4°C and then RIP-lysis buffer for 5 min at 4°C. The co-precipitated RNAs were purified using phenol:chloroform:isoamyl alcohol and subjected to RT-qPCR.

In vivo model. BALB/c nude mice (5-w-old, male) from Shanghai Lab. Animal Co. were used. A tumor-bearing model was constructed by subcutaneously injecting BGC-823 cells transduced with PRAKK1 shRNA. NAC was administered at 150 mg/kg body weight by intraperitoneal injection every other day (n=6/group). Tumor size was monitored every 3 d, and xenografts were collected for terminal deoxynucleotidyl transferase dUTP nick-end labeling (TUNEL) assay. For the survival analysis, a total of 60 mice were used (n=20/group). This study was authorized by the Ethics Committee of Xuzhou Central Hospital.

Data analysis. Three independent replicates were performed for all assays. Data were expressed as mean ± SD. Differences were analyzed by Prism8.4.2 (GraphPad) with Student's t-test or ANOVA. A p-value <0.05 was defined as statistically significant.

Results

PRKAA1 knockdown inhibited cell viability, colony formation, glycolysis, and enhanced apoptosis in GC cells.

To study the role of PRKAA1 in the growth and apoptosis of GC cells, we successfully silenced PRKAA1 (Figure S1A). Compared to silencing control (shNC), the silencing of PRKAA1 suppressed viability (Figure 1A), inhibited colony formation (Figure 1B), promoted apoptosis (Figure 1C), suppressed ECAR (Figure 1D), and decreased lactic acid levels (Figure 1E). Together, these results showed that silencing PRKAA1 suppressed viability, colony formation, and glycolysis but promoted apoptosis of GC cells.

PRKAA1 knockdown inhibited redox balance in GC cells. We then further analyzed the effect of PRKAA1 silencing on redox balance in GC cells. Results suggested that the silencing PRKAA1 significantly increased ROS levels (Figures 2A, 2B). Silencing PRKAA1 also dramatically decreased GSH levels (Figure 2C) but enhanced the NADP⁺/NADPH ratios (Figure 2D). All these findings demonstrated that PRKAA1 knockdown disturbed redox balance in GC cells.

PRKAA1 overexpression enhanced viability, colony formation, glycolysis, and redox balance but inhibited apoptosis. To further explore the role of PRKAA1, we overexpressed PRKAA1 in GC cells (Supplementary Figure S1A). Data showed that compared with control cells, overexpressing PRKAA1 significantly increased cell viability (Figure 3A),

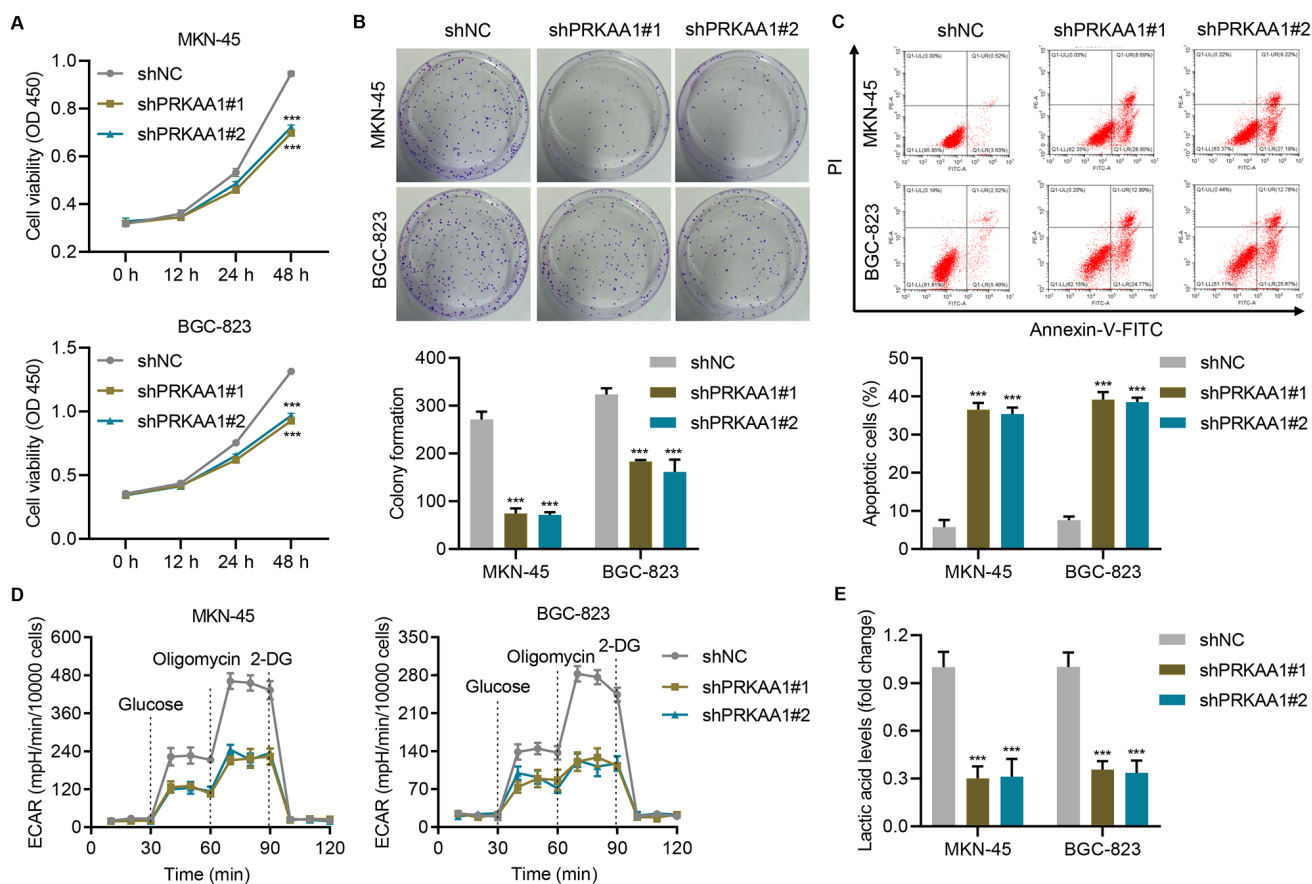


Figure 1. PRKAA1 knockdown inhibited viability, colony formation, and glycolysis but enhanced apoptosis. A) Viability, B) colony formation, C) apoptosis, D) ECAR, and E) lactic acid of GC cells with or without PRKAA1 knockdown. ***p<0.001 vs. shNC

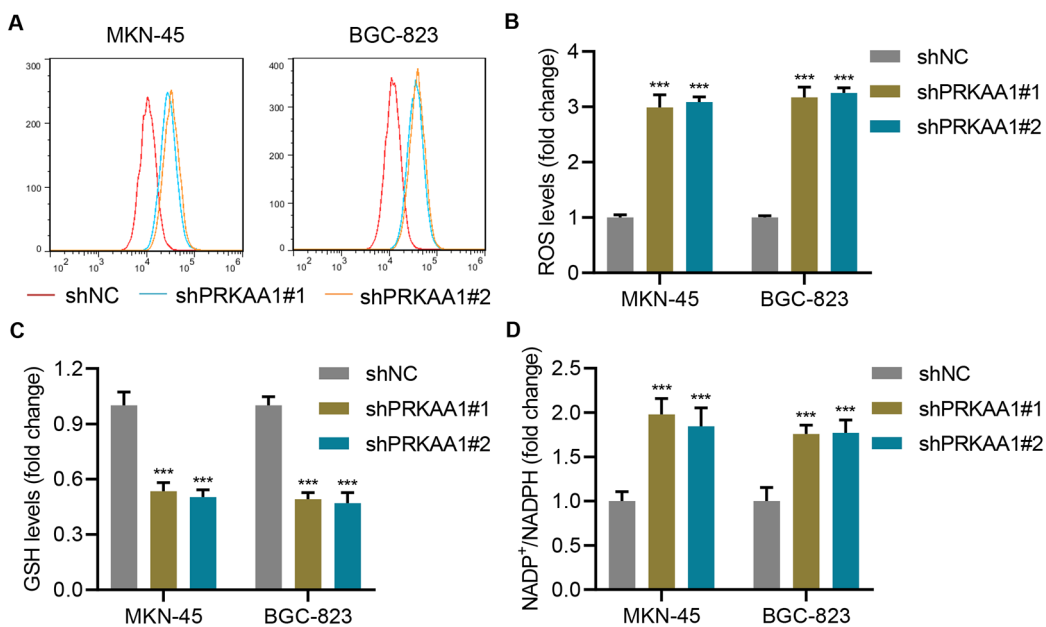


Figure 2. PRKAA1 knockdown suppressed the redox balance. A, B) ROS production, C) GSH, and D) NADP⁺/NADPH ratio of GC cells with or without PRKAA1 knockdown. ***p<0.001 vs. shNC

promoted colony formation (Figure 3B), decreased cell apoptosis (Figure 3C), and increased ECAR (Figure 3D), and lactic acid levels (Figure 3E). Overexpression of PRKAA1 also significantly decreased ROS levels (Figure 3F), increased GSH levels (Figure 3G) but suppressed the NADP⁺/NADPH ratio of GC cells (Figure 3H). These results indicated that PRKAA1 overexpression enhanced viability, colony formation, glycolysis, and redox balance but inhibited apoptosis.

PRKAA1 knockdown suppressed viability, colony formation, and glycolysis but promoted apoptosis by regulating the redox balance. To study how PRKAA1 functions, we introduced NAC (ROS inhibitor). Our results indicated that administration of NAC significantly ameliorated the silencing PRKAA1-caused decrease of cell viability (Figure 4A), inhibition of colony formation (Figures 4B, 4C), increase of apoptosis (Figures 4D, 4E), suppression of

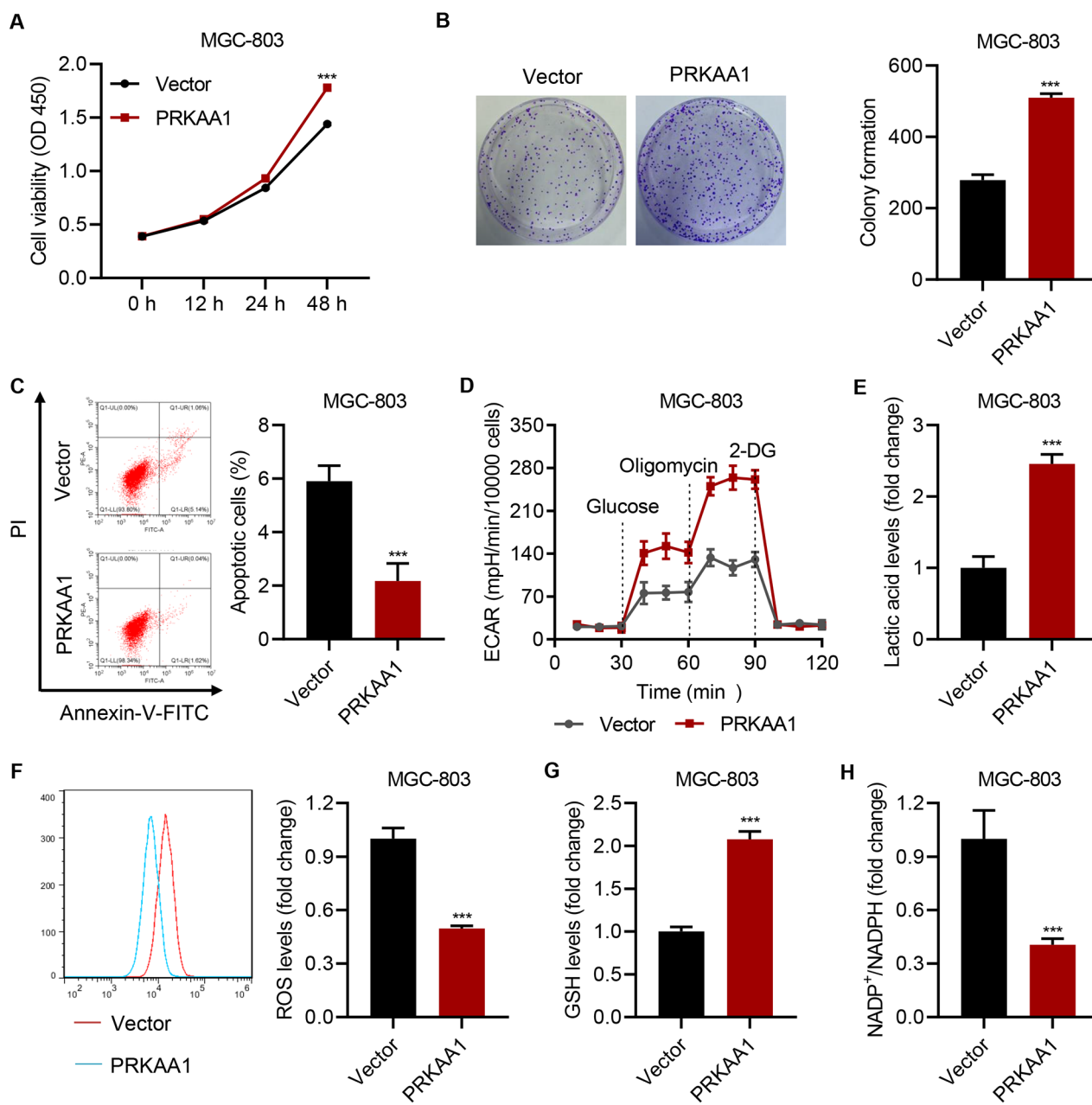


Figure 3. PRKAA1 overexpression enhanced viability, colony formation, glycolysis, and redox balance but inhibited apoptosis. A) Viability, B) colony formation, C) apoptosis, D) ECAR, E) lactic acid, F) ROS production, G) GSH, and H) NADP⁺/NADPH ratio of MGC-803 cells with or without PRKAA1 overexpression. ***p<0.001 vs. Vector

ECAR (Figure 4F), decrease of lactic acid levels (Figure 4G), increases of ROS levels (Figure 4H), and suppression of GSH levels (Figure 4I). Together, the data suggested that the PRKAA1 knockdown suppressed viability, and glycolysis but promoted apoptosis by regulating the redox balance.

PRKAA1 knockdown inhibited tumor growth *in vivo* by regulating redox balance. We then further investigated the effect of PRKAA1 in animals. After inoculation of PRKAA1-silenced BGC-823 cells, NAC or vehicle was administered at a dose of 150 mg/kg body weight by intraperitoneal injection every other day. Silencing of PRKAA1 significantly decreased tumor volume (Figure 5A), tumor weight (Figure 5B), increased tumor apoptosis (Figure 5C), decreased levels of lactic acid (Figure 5D) and GSH (Figure 5E), which were all ameliorated by the administration of NAC. The administration of NAC also significantly ameliorated the silencing-PRKAA1-caused increase of the survival rate (Figure 5F). These findings indicated that PRKAA1 knockdown inhibited tumor growth *in vivo* by regulating the redox balance.

FTO regulated PRKAA1 mRNA m⁶A modification and stability. Because FTO-regulation of m⁶A has been shown to be involved in different biological processes, we

wanted to check whether FTO regulates PRKAA1 mRNA m⁶A modification. FTO was successfully overexpressed or silenced (Supplementary Figure S1B). Silencing FTO significantly increased m⁶A level, while overexpressing FTO significantly decreased m⁶A level (Figure 6A). Silencing FTO also significantly increased m⁶A level of PRKAA1 3'-UTR, while overexpressing FTO significantly decreased m⁶A level of PRKAA1 3'-UTR (Figure 6B). Silencing FTO significantly decreased the luciferase activity of PRKAA1 3'-UTR, while overexpressing FTO significantly increased it (Figure 6C). Silencing FTO also remarkably decreased PRKAA1, while overexpressing FTO significantly increased PRKAA1 at both mRNA and protein levels (Figures 6D, 6E). Silencing FTO significantly decreased the stability of PRKAA1 mRNA (Figure 6F), while silencing YTHDF2 (Supplementary Figure S1C) significantly increased the expression levels of PRKAA1 (Figure 6G, 6H) and increased the stability of PRKAA1 mRNA (Figure 6I). RIP followed by quantitative RT-qPCR assay results showed that there was an interaction between YTHDF2 and PRKAA1 3'-UTR (Figure 6J). Together, these findings demonstrated that FTO regulated PRKAA1 mRNA m⁶A modification and stability.

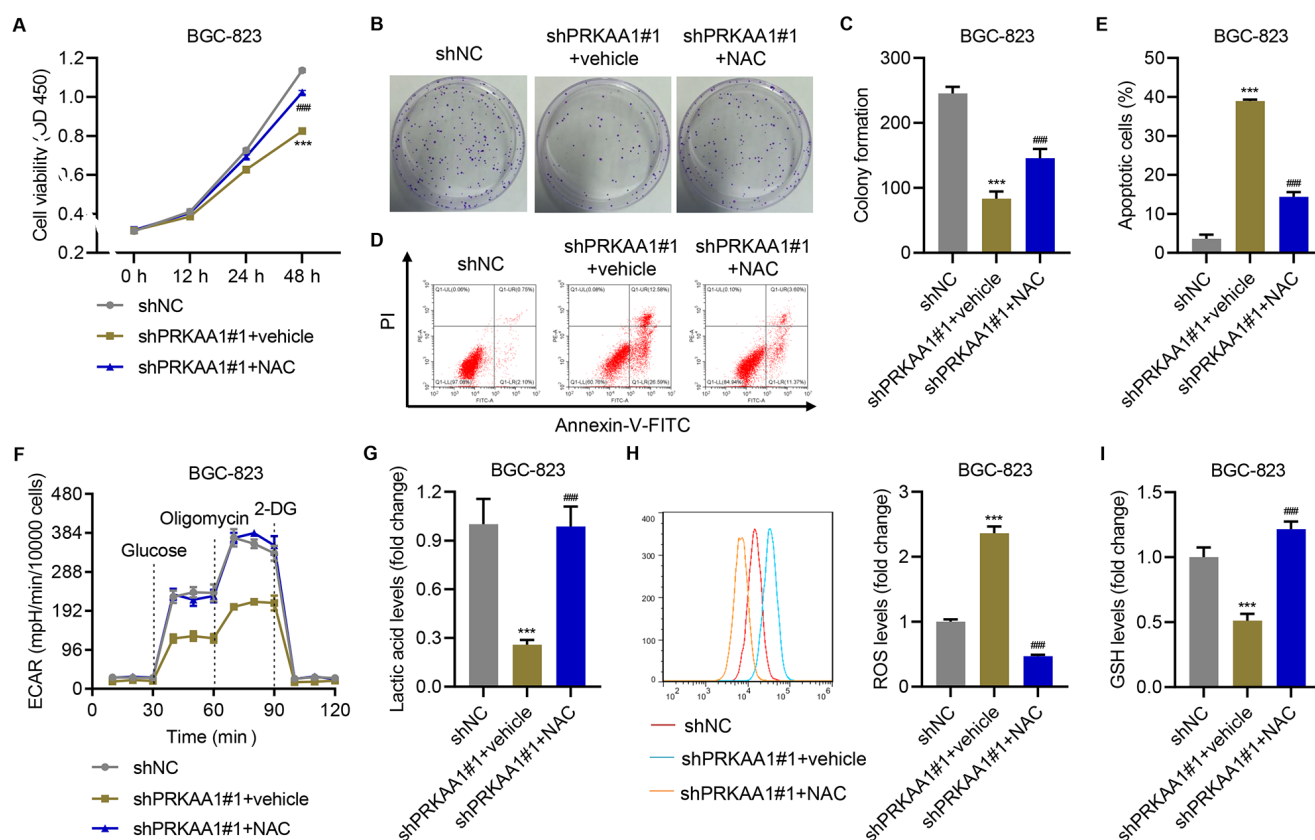


Figure 4. PRKAA1 knockdown inhibited viability, colony formation, and glycolysis but suppressed apoptosis by inhibiting the redox balance. A) Viability, B, C) colony formation, D, E) apoptosis, F) ECAR, G) lactic acid, H) ROS production, and I) GSH of BGC-823 cells with PRKAA1 overexpression and NAC treatment. *** $p < 0.001$ vs. shNC; ### $p < 0.001$ vs. shPRKAA1+vehicle

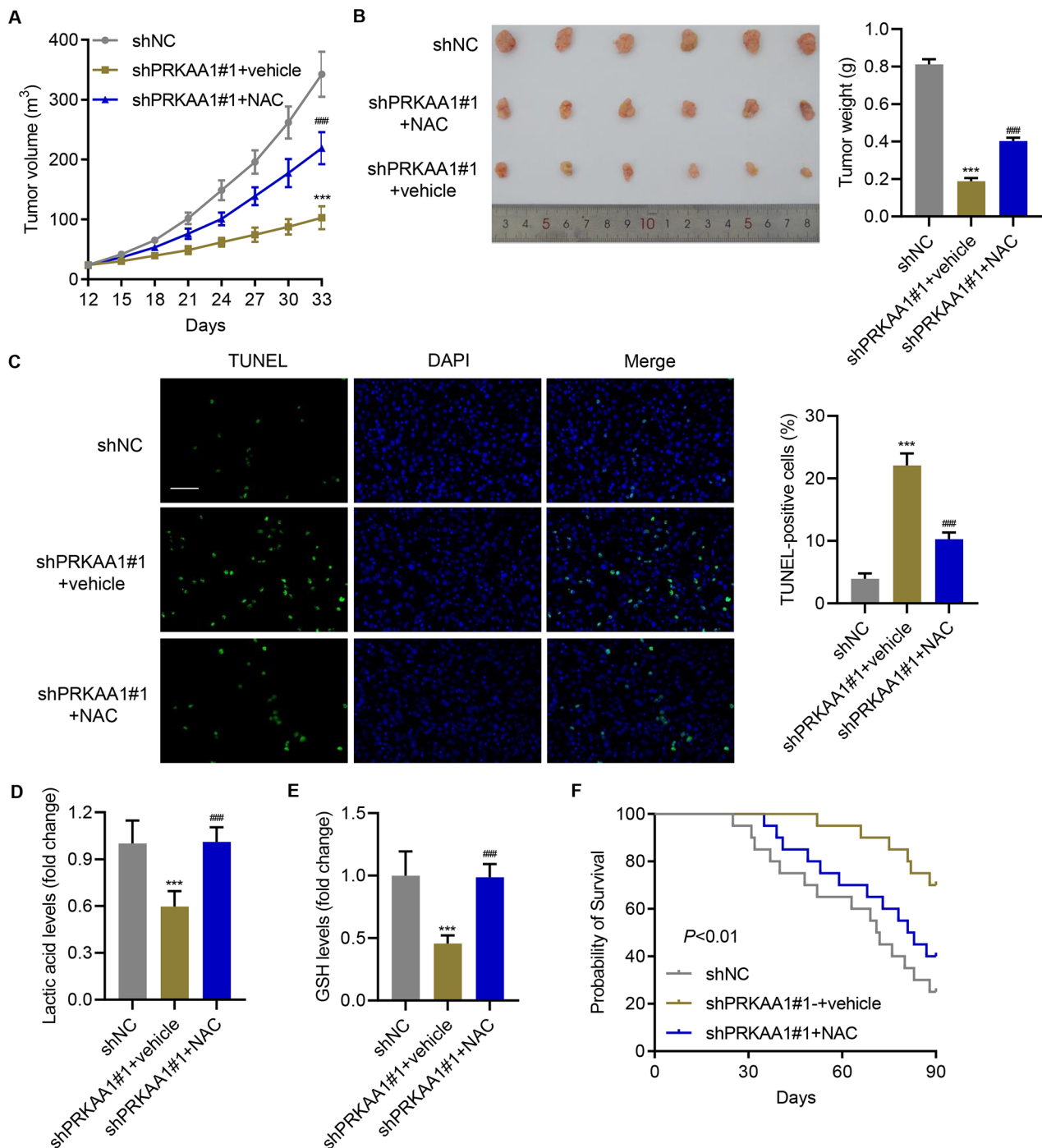


Figure 5. PRKAA1 knockdown suppressed tumor growth by inhibiting the redox balance *in vivo*. BGC-823 cells with/without PRKAA1 silencing were inoculated into the armpits of nude mice with or without NAC treatment. A) Tumor volume, B) tumor weight, C) TUNEL staining, D) GSH, and E) lactic acid levels in tumor xenograft. Scale bar = 50 mm. F) Survival analysis. *** $p < 0.001$ vs. shNC; ### $p < 0.001$ vs. shPRKAA1+vehicle

PRKAA1 and FTO expression in GC tissues and correlation analyses. Next, levels of PRKAA1 and FTO in tumor tissues from the hospital cohort were checked. Data showed that PRKAA1 and FTO mRNA levels (Figures 7A, 7B) were remarkably enhanced in tumors. Data also showed that there

was a significant correlation between PRKAA1 mRNA and FTO mRNA in GC tissues (Figure 7C). We also performed IHC staining of PRKAA1 and FTO using GC tissue microarray (Figure 7D) and found that high levels of PRKAA1 were correlated with high levels of FTO, and low levels of PRKAA1

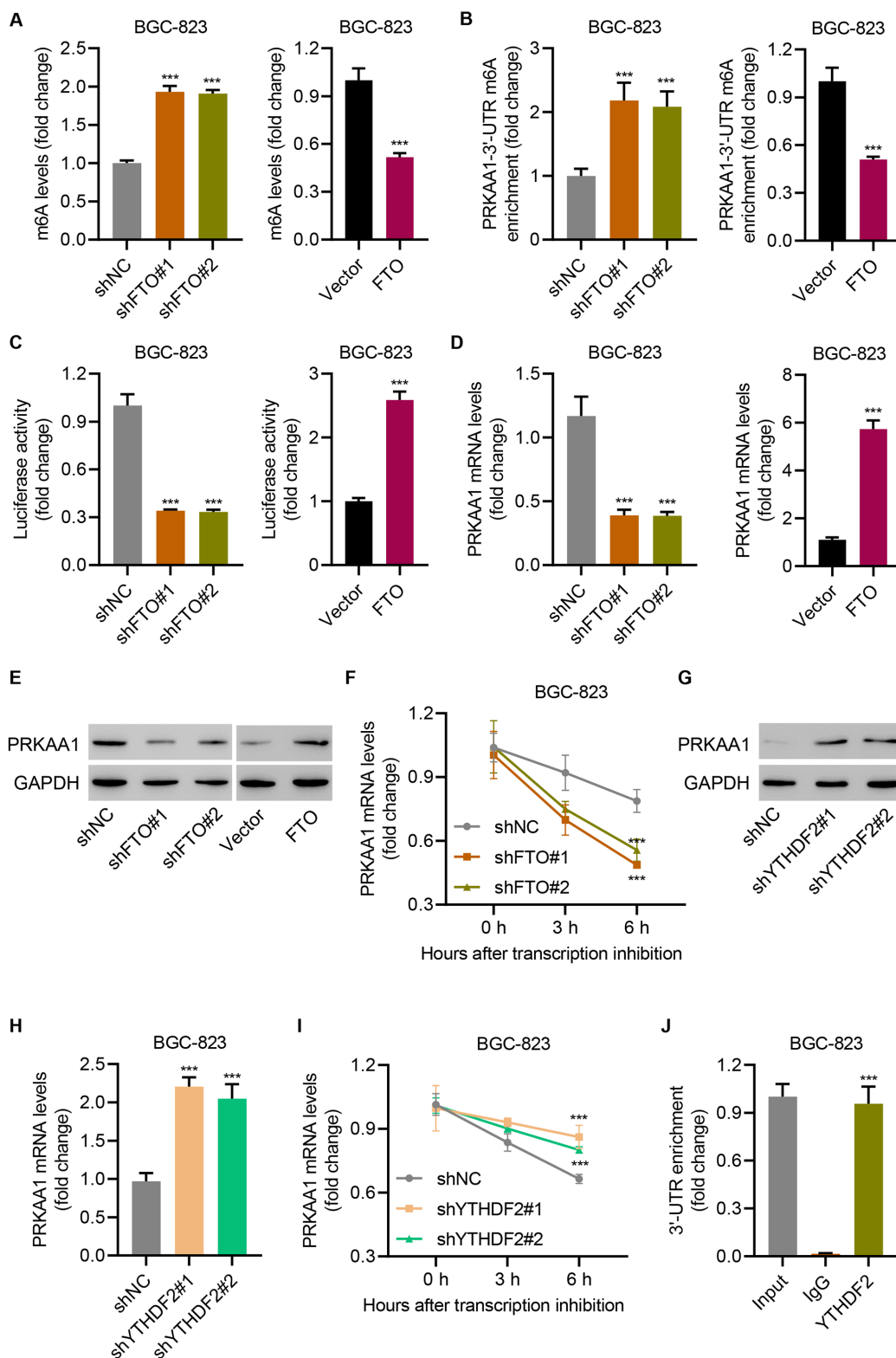


Figure 6. FTO regulated PRKAA1 mRNA m⁶A modification and stability. FTO was silenced in BGC-823 cells. A) The global m⁶A level, B) relative m⁶A levels of PRKAA1 3'-UTR, C) luciferase activity of PRKAA1 3'-UTR, D) mRNA and E) protein of PRKAA1, and F) PRKAA1 mRNA stability were measured. G) Protein and H) mRNA of PRKAA1 expression and I) PRKAA1 mRNA stability in BGC-823 cells transfected with the YTHDF2 shRNA vector. J) RIP followed by RT-qPCR was used to examine the interaction between YTHDF2 and PRKAA1 3'-UTR. ***p<0.001 vs. shNC, vector, or IgG

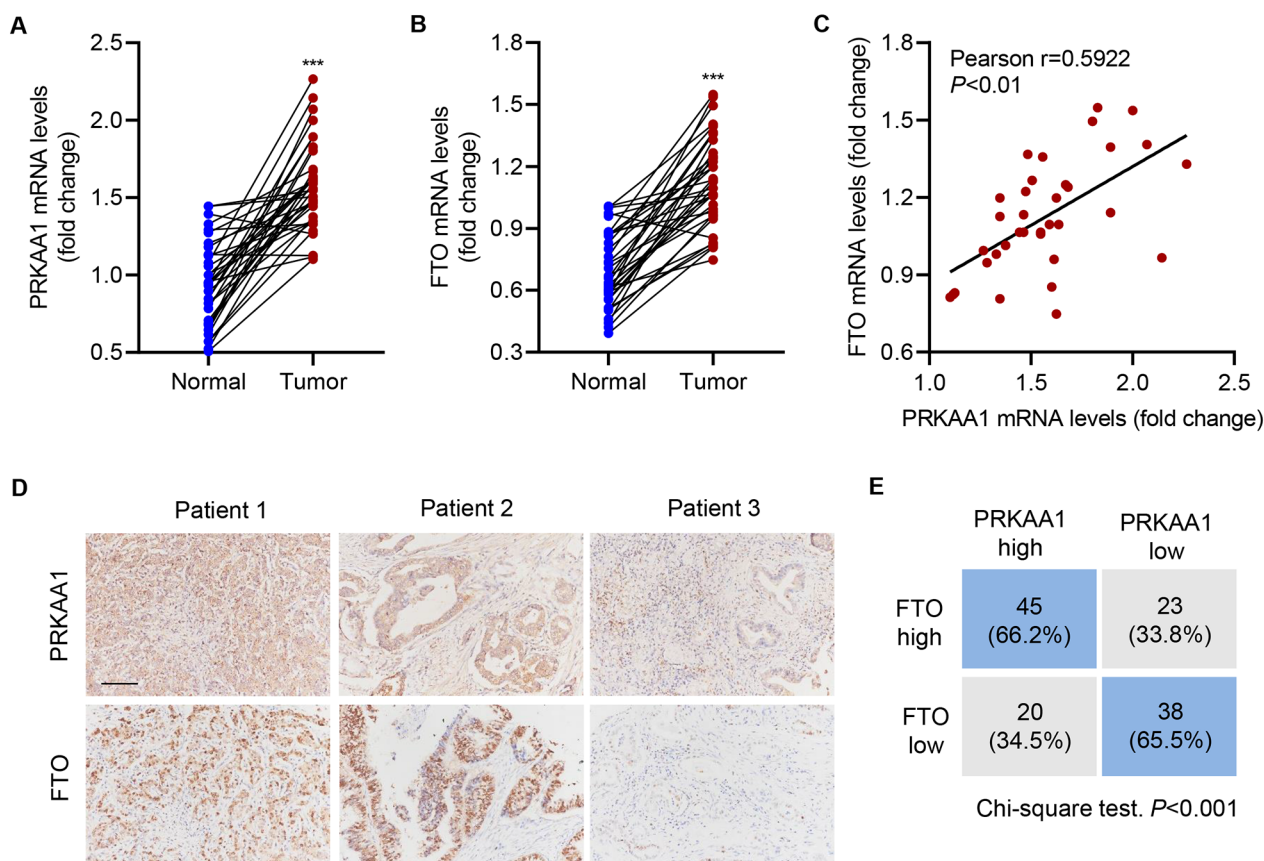


Figure 7. PRKAA1 and FTO levels in GC tissues and their correlation. Levels of A) PRKAA1 and B) FTO in GC or adjacent normal tissues collected from the hospital cohort. C) Correlation scatterplots of GC tissues in a hospital cohort. D) Protein levels of PRKAA1 and FTO of GC tissue microarray. Scale bar = 100 μ m. E) Statistical analysis of GC tissues under various staining conditions

were correlated with low levels of FTO (Figure 7E). All these findings indicated that PRKAA1 and FTO were increased in GC and there was a significant correlation between PRKAA1 and FTO.

Discussion

Our data demonstrated that silencing PRKAA1 suppressed viability, colony formation, and glycolysis but promoted apoptosis of GC cells, whereas overexpressing PRKAA1 promoted viability and glycolysis but decreased apoptosis through regulating the redox balance. Mechanism study indicated that FTO regulated PRKAA1 mRNA m^6A modification and stability. For the first time, our study indicated that FTO increased levels of PRKAA1 by regulating its mRNA m^6A modification. PRKAA1, in turn, promoted cell viability, colony formation, and glycolysis but inhibited apoptosis of GC cells by regulating the redox balance.

Tumor cells convert most glucose to pyruvate even in the presence of oxygen [24]. Metabolic changes may benefit tumor proliferation and growth by providing sufficient

energy and substrates. Chen et al. found that glycolysis and lactic acid were significantly elevated in GC patients [25]. Kogure et al. reported that high metastatic GC cells prefer aerobic glycolysis [26]. Elevated aerobic glycolysis was observed in chemoresistant GC cells [27]. Our data indicated that PRKAA1 overexpression significantly increased viability, colony formation, glycolysis, and lactic acid release but inhibited apoptosis. These findings not only increase our knowledge of the role of PRKAA1 in glycolysis but also broaden our understanding of the progression of GC.

ROS-mediated redox signaling plays a very important role in a variety of biological processes. However, elevated ROS may damage cells [28]. Therefore, redox balance is very critical. ROS may cause DNA mutations to transform normal cells into cancerous cells [29]. Dysregulation of redox balance is involved in various types of cancers. Wang et al. showed that PRKAA1 promoted colorectal cancer cells' survival by promoting the redox balance [30]. Our results indicated that the overexpression of PRKAA1 significantly promoted glycolysis, decreased ROS levels, and increased GSH levels but suppressed the $NADP^+/NADPH$ ratio of GC cells. *In*

in vivo data showed that the administration of NAC significantly ameliorated the silencing-PRKAA1-caused increase of survival rate. These findings indicated that PRKAA1 knock-down inhibited tumor growth by inhibiting redox balance. Previous studies have reported that PRKAA1 downregulates ROS levels by regulating thioredoxin in non-small cell lung cancer [31] and maintains ROS at low levels through the regulation of phosphorylation of glutathione synthesis reductase in colorectal cancer cells [30]. Moreover, ROS inhibits glycolysis by downregulation GLUT1 through the PI3K/AKT signaling pathway in renal cancer cells [32]. These data indicate the possible molecular mechanisms by which PRKAA1 regulates glycolytic pathway/redox balance in GC cells.

Increasing evidence suggests that m⁶A is involved in tumor progression [33]. FTO-regulation of m⁶A is involved in different biological processes. For instance, FTO-mediated demethylation of m⁶A is involved in lipid metabolism in skeletal muscle cells [16]. In our study, we revealed a new role of FTO/m⁶A modification of PRKAA1 in GC, which may improve our understanding of the possible mechanism by which PRKAA1 regulates GC progression.

There are some limitations in our study. To further study the role of PRKAA1/glycolysis in GC, future research using PDX models may find more interesting data. More GC cells should be included to investigate whether the results observed are cell line specific. Although shortcomings are there, the study reveals a novel mechanism by which PRKAA1/glycolysis regulates GC progression.

In conclusion, our data revealed a novel function of the PRKAA1/glycolysis axis, suggesting that FTO-mediated PRKAA1 m⁶A modification, leading to the upregulation of PRKAA1, which promoted cell viability, colony formation, and glycolysis but inhibited the apoptosis of GC cells by promoting redox balance. The findings highlighted the importance of PRKAA1 signaling, which may lay the foundation for new therapeutics for GC treatments.

Supplementary information is available in the online version of the paper.

Acknowledgments: This study was funded by the Natural Science Foundation of Jiangsu Province (BK20201153), National Natural Science Foundation of China (No.81502435), 2020 Top talent project of “Six and one Project” for high-level health talents (LGY2020029), and the Social Development Project of Xuzhou City (KC20156).

References

- [1] SITARZ R, SKIERUCHA M, MIELKO J, OFFERHAUS GJA, MACIEJEWSKI R et al. Gastric cancer: epidemiology, prevention, classification, and treatment. *Cancer Manag Res* 2018; 10: 239–248. <https://doi.org/10.2147/CMAR.S149619>
- [2] CARCAS LP. Gastric cancer review. *J Carcinog* 2014; 13: 14. <https://doi.org/10.4103/1477-3163.146506>
- [3] AJANI JA, LEE J, SANO T, JANJIGIAN YY, FAN D et al. Gastric adenocarcinoma. *Nat Rev Dis Primers* 2017; 3: 17036. <https://doi.org/10.1038/nrdp.2017.36>
- [4] SEXTON RE, AL HALLAK MN, DIAB M, AZMI AS. Gastric cancer: a comprehensive review of current and future treatment strategies. *Cancer Metastasis Rev* 2020; 39: 1179–1203. <https://doi.org/10.1007/s10555-020-09925-3>
- [5] STAHL P, SEESCHAAF C, LEBOK P, KUTUP A, BOCKHORN M et al. Heterogeneity of amplification of HER2, EGFR, CCND1 and MYC in gastric cancer. *BMC gastroenterol* 2015; 15: 7. <https://doi.org/10.1186/s12876-015-0231-4>
- [6] JOSHI SS, BADGWELL BD. Current treatment and recent progress in gastric cancer. *CA Cancer J Clin* 2021; 71: 264–279. <https://doi.org/10.3322/caac.21657>
- [7] LIU W, ZHAO ZM, LIU YL, PAN HF, LIN LZ. Weipiling ameliorates gastric precancerous lesions in Atp4a(–/–) mice. *BMC Complement Altern Med* 2019; 19: 318. <https://doi.org/10.1186/s12906-019-2718-y>
- [8] SHI XJ, YU B, WANG JW, QI PP, TANG K et al. Structurally novel steroidal spirooxindole by241 potently inhibits tumor growth mainly through ROS-mediated mechanisms. *Sci Rep* 2016; 6: 31607. <https://doi.org/10.1038/srep31607>
- [9] PIZZIMENTI S, RIBERO S, CUCCI MA, GRATAROLA M, MONGE C et al. Oxidative Stress-Related Mechanisms in Melanoma and in the Acquired Resistance to Targeted Therapies. *Antioxidants* 2021; 10: 1942. <https://doi.org/10.3390/antiox10121942>
- [10] HARDIE DG. The AMP-activated protein kinase pathway--new players upstream and downstream. *J Cell Sci* 2004; 117: 5479–5487. <https://doi.org/10.1242/jcs.01540>
- [11] ZHU H, FORETZ M, XIE Z, ZHANG M, ZHU Z et al. PRKAA1/AMPK α 1 is required for autophagy-dependent mitochondrial clearance during erythrocyte maturation. *Autophagy* 2014; 10: 1522–1534. <https://doi.org/10.4161/auto.29197>
- [12] CHEN M, JIANG B, HE B, TANG M, WANG P et al. Genetic variations in PRKAA1 predict the risk and progression of gastric Cancer. *BMC Cancer* 2018; 18: 923. <https://doi.org/10.1186/s12885-018-4818-3>
- [13] CHEN W, JI Y. CircC6orf132 Facilitates Proliferation, Migration, Invasion, and Glycolysis of Gastric Cancer Cells Under Hypoxia by Acting on the miR-873-5p/PRKAA1 Axis. *Front Genet* 2021; 12: 636392. <https://doi.org/10.3389/fgene.2021.636392>
- [14] ZHANG Y, ZHOU X, CHENG L, WANG X, ZHANG Q et al. PRKAA1 Promotes Proliferation and Inhibits Apoptosis of Gastric Cancer Cells Through Activating JNK1 and Akt Pathways. *Oncol Res* 2020; 28: 213–223. <https://doi.org/10.3727/096504019X15668125347026>
- [15] ZHANG Y, ZHOU X, ZHANG Q, ZHANG Y, WANG X et al. Involvement of NF- κ B signaling pathway in the regulation of PRKAA1-mediated tumorigenesis in gastric cancer. *Artif Cells Nanomed Biotechnol* 2019; 47: 3677–3686. <https://doi.org/10.1080/21691401.2019.1657876>

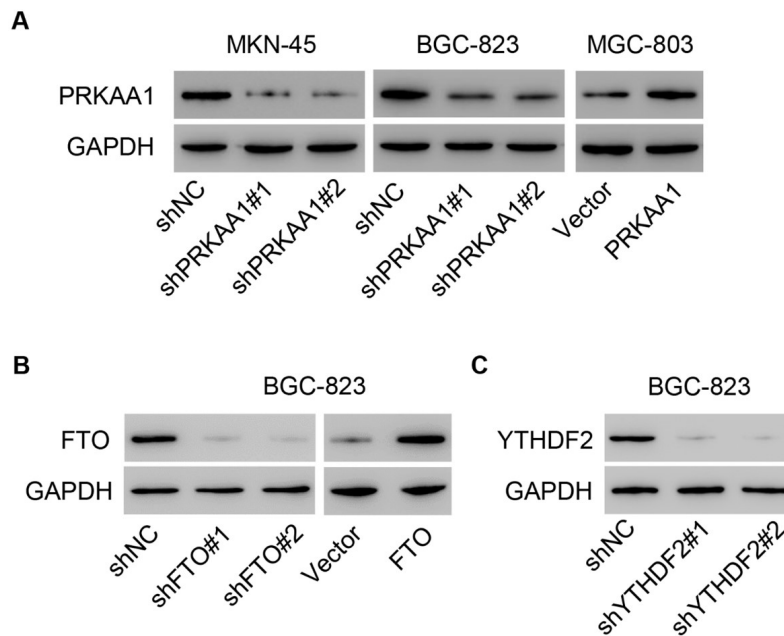
- [16] WU W, FENG J, JIANG D, ZHOU X, JIANG Q et al. AMPK regulates lipid accumulation in skeletal muscle cells through FTO-dependent demethylation of N(6)-methyladenosine. *Sci Rep* 2017; 7: 41606. <https://doi.org/10.1038/srep41606>
- [17] RUUD J, ALBER J, TOKARSKA A, ENGSTROM RUUD L, NOLTE H et al. The Fat Mass and Obesity-Associated Protein (FTO) Regulates Locomotor Responses to Novelty via D2R Medium Spiny Neurons. *Cell Rep* 2019; 27: 3182–3198 e9. <https://doi.org/10.1016/j.celrep.2019.05.037>
- [18] YANG X, HU X, LIU J, WANG R, ZHANG C et al. N6-methyladenine modification in noncoding RNAs and its function in cancer. *Biomark Res* 2020; 8: 61. <https://doi.org/10.1186/s40364-020-00244-x>
- [19] YIN H, ZHANG X, YANG P, ZHANG X, PENG Y et al. RNA m6A methylation orchestrates cancer growth and metastasis via macrophage reprogramming. *Nat Commun* 2021; 12: 1394. <https://doi.org/10.1038/s41467-021-21514-8>
- [20] ZHANG D, NING J, OKON I, ZHENG X, SATYANARAYANA G et al. Suppression of m6A mRNA modification by DNA hypermethylated ALKBH5 aggravates the oncological behavior of KRAS mutation/LKB1 loss lung cancer. *Cell Death Dis* 2021; 12: 518. <https://doi.org/10.1038/s41419-021-03793-7>
- [21] YANG S, WEI J, CUI YH, PARK G, SHAH P et al. m(6)A mRNA demethylase FTO regulates melanoma tumorigenicity and response to anti-PD-1 blockade. *Nat Commun* 2019; 10: 2782. <https://doi.org/10.1038/s41467-019-10669-0>
- [22] CRIBBS AP, KENNEDY A, GREGORY B, BRENNAN FM. Simplified production and concentration of lentiviral vectors to achieve high transduction in primary human T cells. *BMC Biotech* 2013;13: 98. <https://doi.org/10.1186/1472-6750-13-98>
- [23] GUO Y, LIANG F, ZHAO F, ZHAO J. Resibufogenin suppresses tumor growth and Warburg effect through regulating miR-143-3p/HK2 axis in breast cancer. *Mol Cell Biochem* 2020; 466: 103–115. <https://doi.org/10.1007/s11010-020-03692-z>
- [24] MARBANIANG C, KMA L. Dysregulation of Glucose Metabolism by Oncogenes and Tumor Suppressors in Cancer Cells. *Asian Pac J Cancer Prev* 2018; 19: 2377–2390. <https://doi.org/10.22034/APJCP.2018.19.9.2377>
- [25] CHEN JL, FAN J, LU XJ. CE-MS based on moving reaction boundary method for urinary metabolomic analysis of gastric cancer patients. *Electrophoresis* 2014; 35: 1032–1039. <https://doi.org/10.1002/elps.201300243>
- [26] KOGURE A, NAITO Y, YAMAMOTO Y, YASHIRO M, KIYONO T et al. Cancer cells with high-metastatic potential promote a glycolytic shift in activated fibroblasts. *PLoS One* 2020; 15: e0234613. <https://doi.org/10.1371/journal.pone.0234613>
- [27] QIAN X, XU W, XU J, SHI Q, LI J et al. Enolase 1 stimulates glycolysis to promote chemoresistance in gastric cancer. *Oncotarget* 2017; 8: 47691–4708. <https://doi.org/10.18632/oncotarget.17868>
- [28] KONG H, CHANDEL NS. Regulation of redox balance in cancer and T cells. *The J Biol Chem* 2018; 293: 7499–7507. <https://doi.org/10.1074/jbc.TM117.000257>
- [29] PUROHIT V, SIMEONE DM, LYSSIOTIS CA. Metabolic Regulation of Redox Balance in Cancer. *Cancers* 2019; 11: 955. <https://doi.org/10.3390/cancers11070955>
- [30] WANG YN, LU YX, LIU J, JIN Y, BI HC et al. AMPK α 1 confers survival advantage of colorectal cancer cells under metabolic stress by promoting redox balance through the regulation of glutathione reductase phosphorylation. *Oncogene* 2020; 39: 637–650. <https://doi.org/10.1038/s41388-019-1004-2>
- [31] GONG D, LI Y, WANG Y, CHI B, ZHANG J et al. AMPK α 1 Downregulates ROS Levels Through Regulating Trx Leading to Dysfunction of Apoptosis in Non-Small Cell Lung Cancer. *Onco Targets Ther* 2020; 13: 5967–5977. <https://doi.org/10.2147/ott.S236235>
- [32] WANG KJ, MENG XY, CHEN JF, WANG KY, ZHOU C et al. Emodin Induced Necroptosis and Inhibited Glycolysis in the Renal Cancer Cells by Enhancing ROS. *Oxid Med Cell Longev* 2021; 2021: 8840590. <https://doi.org/10.1155/2021/8840590>
- [33] YANG C, HU Y, ZHOU B, BAO Y, LI Z et al. The role of m(6)A modification in physiology and disease. *Cell Death Dis* 2020; 11: 960. <https://doi.org/10.1038/s41419-020-03143-z>

https://doi.org/10.4149/neo_2022_220714N714

PRKAA1, stabilized by FTO in an m6A-YTHDF2-dependent manner, promotes cell proliferation and glycolysis of gastric cancer by regulating the redox balance

Yangmei ZHANG^{1,2,3,4,*}, Xichang ZHOU^{5,*}, Xue CHENG^{6,*}, Xiou HONG⁷, Xiaowei JIANG⁸, Guilong JING⁸, Kai CHEN^{1,*}, Yang LI^{7,*}

Supplementary Information



Supplementary Figure S1. The protein levels of A) PRKAA1, B) FTO and C) YTHDF2 in gastric cancer cells (MKN-45, BGC-823 and MGC-803) transfected with indicated vectors.